A General Noise De-embedding Procedure for Packaged Two-Port Linear Active Devices

Robert A. Pucel, *Life Fellow, IEEE,* Wayne Struble, Robert Hallgren *Member, IEEE,* and Ulrich L. Rohde

Abstract—**A general noise de-embedding procedure is described for packaged two-port linear active devices. The method is based on the noise correlation technique and its applications developed previously [1]–[3]. In its most general form, the package, which need not be reciprocal, may consist of an arbitrary interconnection of linear passive elements at thermal equilibrium. Only the terminal admittance properties of the package need be known, not its topology. However, under certain special cases which lead to singular submatrices of the admittance matrix the method is inapplicable as will be pointed out. This situation may occur when elements such as isolators are part of the package. Our objective in this paper is to draw together, in one place, the necessary theoretical foundation and experimental techniques to enable workers, not familiar with the field, to assemble the software and laboratory setup for two-port noise de-embedding. In line with this objective, we have borrowed from the work of earlier authors [2], [4]. In furtherance of our goal to make the paper self-contained, we describe in some detail the automated noise measurement system used for data acquisition and the mathematical basis for it. Last, but not least, we establish the validity of the de-embedding approach with extensive experimental data obtained on three MESFETs and a PsHEMT.**

Introduction

TWO-PORT active devices, for example, FETs are being used in microwave circuits such as MMICs over a wide frequency spectrum extending from *L*-band well into the millimeter band ($f > 30$ GHz). Many of these circuits are broadband amplifiers with octave or greater bandwidth. In order to design such amplifiers one must characterize not only the small-signal amplifying properties of the device, but also the noise properties. Equivalent circuit models of, say, the FET, especially the GaAs variety, have now been characterized with sufficient accuracy up to at least 40 GHz. However, this is not the case for the noise properties, one reason being the difficulty of performing accurate noise measurements in the millimeter band, another being the sheer amount of experimental data necessary for obtaining accurate noise data over a large frequency band because of the redundancy required for least squares fitting to the four noise parameters of the active device.

It is evident that there is a need for a broadband noise model which can be based on a minimal set of noise measurements at a convenient frequency in the microwave band, such as, for example, 10 GHz. Indeed, a model based on a single frequency set of measurements would be ideal, since a standardized measurement procedure utilizing fully characterized source impedances (source pull), preferably, automated could be implemented.

We describe a mathematical technique to predict the noise performance of an active linear two-port over its entire frequency range of operation based on the characterization of the four noise parameters at a single frequency. The technique is applicable to any two-port and is ideal for computer aided design systems. As examples of the method, several FET devices will be analyzed.

The method is a noise de-embedding scheme which allows one to predict the noise properties of a packaged device at any frequency given the values of the four noise parameters at a single frequency, the equivalent circuit model of the active two-port, and the four port y (or *S*) parameters of the package. The algorithm applies to an arbitrary package topology. Linearity, passivity, and thermal equilibrium are the only conditions imposed on the package. A key assumption underlying the method is that the *frequency* dependence of all relevant noise sources is known, including their correlation. The de-embedding technique establishes the magnitude of the noise sources at the measurement frequency, and hence, by implication, at all other frequencies.

The method is based on the noise power matrix introduced by Haus [1] later renamed the noise correlation matrix by Hillbrand and Russer [2]. The latter demonstrated that the correlation matrix was ideally suited for the analysis of noise in linear two-port circuits by computer aided design techniques and applied the technique to the noise analysis of an n-port network [3]. A similar generalized approach based on the nodal (admittance) technique was advanced by Rizzoli and Lipparini somewhat later [4]. An alternative to the correlation matrix technique was proposed recently by Heinen, *et al.* [5].

Our procedure is an application of the approach described in [4], but now applied to the *de-embedding* problem. The de-embedding application was cited by Rizzoli,

Manuscript received September 3, 1991; revised April 6, 1992.

R. A. Pucel and W. Struble are with Raytheon Company, Research Division, 131 Spring Street, Lexington, MA 02173.

R. Hallgren was with Raytheon Company, Lexington, MA. He is presently with the Electromagnetics Institute, Technical University of Denmark, Lyngby, Denmark.

U. L. Rohde is with Compact Software, Inc., 483 McLean Blvd., Paterson, NJ 07504.

IEEE Log Number 9292893.

et al. [6], though not in sufficient detail for the general user.[1] In this paper we wish to expand on this approach, and provide extensive experimental data to establish its validity. An example of a similar de-embedding technique but restricted to a specific package topology was presented recently by Riddle [7].

Theory

We shall establish in this section, the theoretical basis for the de-embedding scheme by following the mathematical treatment developed in [4] and [6]. In line with the objective of this paper, we have extracted those equations from these two references which are relevant for our purpose. Some obvious changes in nomenclature have been introduced, however.

Let $\boldsymbol{C}_{pd}$ and $\boldsymbol{C}_d$ denote the admittance noise correlation matrices of the packaged device and the device alone, respectively. See Fig. 1. These correlation matrices are related by the linear matrix equation [4]

$$\boldsymbol{C}_{pd} = \boldsymbol{P}\boldsymbol{C}_p\boldsymbol{P}^\dagger + \boldsymbol{D}\boldsymbol{C}_d\boldsymbol{D}^\dagger \tag{1}$$

where $\boldsymbol{C}_p$ denotes the admittance correlation matrix of the package 4-port, and $\boldsymbol{P}$ and $\boldsymbol{D}$ represent package and device transformation matrices expressible in terms of the admittance parameters of the package and device. The dagger denotes the Hermitian (conjugate-transpose) of the associated matrix.

Conversely, the noise matrix of the device can be expressed in terms of the noise matrix of the packaged device [4] by an inversion of (1). Thus we have

$$\boldsymbol{C}_d = \boldsymbol{D}^{-1}(\boldsymbol{C}_{pd} - \boldsymbol{P}\boldsymbol{C}_p\boldsymbol{P}^\dagger)\boldsymbol{D}^{\dagger -1} \tag{2}$$

Equation (1) shows that the noise correlation matrix of the packaged device is a superposition of contributions from the package and the active device. Equation (2) states that given the noise correlation matrix of the packaged device, subtraction of the package contribution from it yields the contribution of the device itself. It is evident that (2) is used for de-embedding, while (1) is used for analysis. Under special conditions the matrix $\boldsymbol{D}$ may not possess an inverse, and the de-embedding procedure fails. This may occur when certain nonreciprocal elements, such as isolators are considered part of the package.

Once the device correlation matrix is de-embedded by specification of the noise properties of the packaged device at a specified frequency, this matrix may be evaluated at some other frequency and inserted in (1) to predict the noise performance of the packaged device at that frequency.

The de-embedding scheme described and represented by (2) yields the device noise properties at its two-port terminals. Generally, de-embedding has to be carried out further into the device to reach the ultimate sources of noise whose frequency dependence is known. This phase of de-embedding, however, is device specific. In the case of FETs, the intrinsic device noise mechanisms can be assumed to be frequency independent ("white") [8].

[1]The procedure to be described is a generalization of a more restrictive de-embedding scheme developed earlier under the MIMIC program which was similar to the approach described in [6].

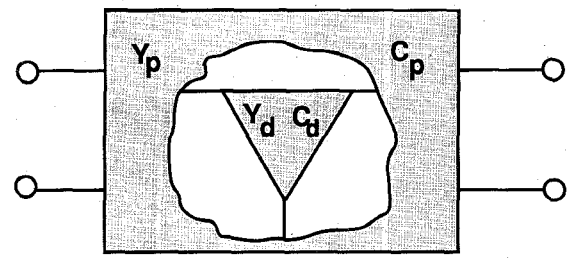

Fig. 1. Relevant to definition of Y-parameter and noise correlation matrices for a packaged two-port.

Analysis

Our goal in this section is to establish the validity of (1) and (2) and to present the expressions for the matrix transformation matrices $\boldsymbol{P}$ and $\boldsymbol{D}$ in terms of the y-parameters of the package and the active device. For this purpose we shall repeat relevant portions of the analysis of [4].

Since the analysis rests heavily on matrix operations, we begin by listing the nomenclature to be used. *All noise correlation matrices are assumed to be in admittance form unless stated otherwise.*

$\boldsymbol{Y}_p$ = four-port admittance matrix of package
$\boldsymbol{Y}_d$ = two-port admittance matrix of active device
$\boldsymbol{Y}_{pd}$ = two-port admittance matrix of packaged device
$\boldsymbol{C}_p$ = noise correlation matrix of package
$\boldsymbol{C}_d$ = noise correlation matrix of active device
$\boldsymbol{C}_{pd}$ = noise correlation matrix of packaged device
$\boldsymbol{N}_p$ = matrix of noise current sources of package
$\boldsymbol{J}_d$ = matrix of noise current sources of active device
$\boldsymbol{I}_k$ = identity matrix of order k

The signal and noise representation of the active device is illustrated in Fig. 2. Note that it is not required that the two ports share a common terminal. The signal and noise model of the package is represented in admittance form in Fig. 3. Fig. 4 is a composite illustration of the device and package. We shall use this figure as a reference for our nodal circuit equation derivations. For clarity and conciseness, we shall present these circuit equations as matrix equations.

We begin with the port voltages and currents. Please refer to Figs. 2–3. Let ports 1–1′ and 2–2′ of the package be denoted as the external ports, and the corresponding voltages and currents as the external voltages and currents. Let ports 3–3′ and 4–4′ denote the internal ports, and the corresponding notation for the voltages and currents. Using the subscripts i and e to designate *internal* and *external* ports, we define the matrices

$$\boldsymbol{V}_e = \begin{bmatrix} V_1 \\ V_2 \end{bmatrix} \quad \boldsymbol{V}_i = \begin{bmatrix} V_3 \\ V_4 \end{bmatrix} \tag{3a}$$

$$\boldsymbol{I}_e = \begin{bmatrix} I_1 \\ I_2 \end{bmatrix} \quad \boldsymbol{I}_i = \begin{bmatrix} I_3 \\ I_4 \end{bmatrix} \tag{3b}$$

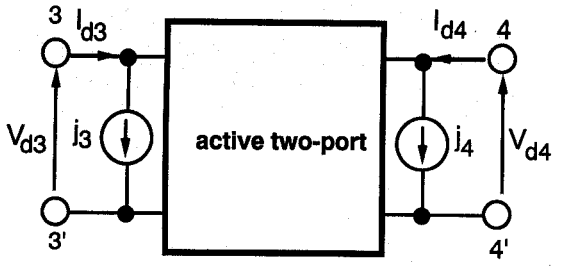

Fig. 2. Signal and noise representation of active two-port.

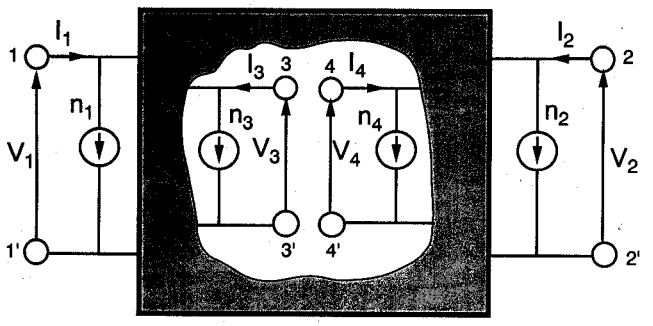

Fig. 3. Signal and noise representation of a package.

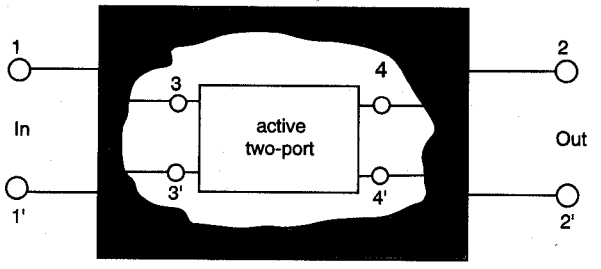

Fig. 4. Package with embedded active two-port device.

and

$$\boldsymbol{V} = \begin{bmatrix} \boldsymbol{V}_e \\ \cdots \\ \boldsymbol{V}_i \end{bmatrix} = \begin{bmatrix} V_1 \\ V_2 \\ \cdots \\ V_3 \\ V_4 \end{bmatrix} \quad \boldsymbol{I} = \begin{bmatrix} \boldsymbol{I}_e \\ \cdots \\ \boldsymbol{I}_i \end{bmatrix} = \begin{bmatrix} I_1 \\ I_2 \\ \cdots \\ I_3 \\ I_4 \end{bmatrix} \tag{4}$$

We also define in a likewise manner the package noise source matrices

$$\boldsymbol{N}_{pe} = \begin{bmatrix} n_1 \\ n_2 \end{bmatrix} \quad \boldsymbol{N}_{pi} = \begin{bmatrix} n_3 \\ n_4 \end{bmatrix} \quad \boldsymbol{N}_p = \begin{bmatrix} \boldsymbol{N}_{pe} \\ \cdots \\ \boldsymbol{N}_{pi} \end{bmatrix} \tag{5}$$

The dotted lines denote partitioning.

We partition the package admittance matrix as

$$\boldsymbol{Y}_p = \begin{bmatrix} \boldsymbol{Y}_{ee} \vdots \boldsymbol{Y}_{ei} \\ \cdots\cdots\cdots \\ \boldsymbol{Y}_{ie} \vdots \boldsymbol{Y}_{ii} \end{bmatrix} \tag{6}$$

where all submatrices are square and of order 2.

The signal and noise nodal equations for the package can be expressed succinctly in terms of the above matrices as follows:

$$\boldsymbol{I} = \boldsymbol{Y}_p \boldsymbol{V} + \boldsymbol{N}_p \tag{7}$$

or in partitioned form as

$$\boldsymbol{I}_e = \boldsymbol{Y}_{ee} \boldsymbol{V}_e + \boldsymbol{Y}_{ei} \boldsymbol{V}_i + \boldsymbol{N}_{pe} \tag{8a}$$

$$\boldsymbol{I}_i = \boldsymbol{Y}_{ie} \boldsymbol{V}_e + \boldsymbol{Y}_{ii} \boldsymbol{V}_i + \boldsymbol{N}_{pi} \tag{8b}$$

We follow a similar procedure for the active device. If $\boldsymbol{I}_d$ and $\boldsymbol{V}_d$ denote the current and voltage matrices for the active device, then we may write the nodal equations for it as

$$\boldsymbol{I}_d = \boldsymbol{Y}_d \boldsymbol{V}_d + \boldsymbol{J}_d \tag{9}$$

where

$$\boldsymbol{I}_d = \begin{bmatrix} I_{d3} \\ I_{d4} \end{bmatrix} \quad \boldsymbol{V}_d = \begin{bmatrix} V_{d3} \\ V_{d4} \end{bmatrix} \quad \boldsymbol{J}_d = \begin{bmatrix} j_3 \\ j_4 \end{bmatrix}. \tag{10}$$

Applying the boundary conditions

$$\boldsymbol{I}_d = -\boldsymbol{I}_i \quad \boldsymbol{V}_d = \boldsymbol{V}_i \tag{11}$$

to (9), inserting the latter into (8b) and solving for $\boldsymbol{V}_i$ we obtain

$$\boldsymbol{V}_i = -(\boldsymbol{Y}_{ii} + \boldsymbol{Y}_d)^{-1}(\boldsymbol{Y}_{ie} \boldsymbol{V}_e + \boldsymbol{N}_{pi} + \boldsymbol{J}_d). \tag{12}$$

Inserting this into (8a) we solve for the two-port signal and noise nodal equations of the packaged device in the concise matrix form as

$$\boldsymbol{I}_e = \boldsymbol{Y}_e \boldsymbol{V}_e + \boldsymbol{I}_n \tag{13}$$

where the first term represents the signal component of current and the second the noise component. Evidently $\boldsymbol{Y}_e$ represents the admittance matrix of the two-port packaged device. It is given by the expression

$$\boldsymbol{Y}_e = \boldsymbol{Y}_{ee} + \boldsymbol{D}\boldsymbol{Y}_{ie} \tag{14}$$

where the matrix $\boldsymbol{D}$ is defined as

$$\boldsymbol{D} = -\boldsymbol{Y}_{ei}(\boldsymbol{Y}_{ii} + \boldsymbol{Y}_d)^{-1}. \tag{15}$$

The noise matrix term $\boldsymbol{I}_n$ denotes the sum of the contributions of the package and active device. This superposition of noise sources is represented succinctly in matrix form as

$$\boldsymbol{I}_n = \boldsymbol{P}\boldsymbol{N}_p + \boldsymbol{D}\boldsymbol{J}_d \tag{16}$$

where

$$\boldsymbol{P} = [\boldsymbol{I}_2 \vdots \boldsymbol{D}] \tag{17}$$

with $\boldsymbol{I}_2$ being the identity matrix of order 2.

We are now in a position to derive the admittance noise correlation matrix of the packaged device. Thus

$$\boldsymbol{C}_{pd} = \overline{\boldsymbol{I}_n \boldsymbol{I}_n^{\dagger}} \tag{18}$$

where the overbar denotes the statistical average.[2] Inserting (16) into (18) and recognizing that no correlation ex-

[2]We point out here that throughout our analysis the statistical noise averages, hence correlation matrices, are normalized (divided by) the factor $2kT_oB$, where k represents Boltzmann's constant, T_o = the standard temperature of 290°K, and B denotes the noise bandwidth, usually assumed to be one Hertz. The factor 2 (instead of 4) implies that we are assuming a frequency scale encompassing both negative and positive values. This normalization was chosen for convenience. In any case, this factor cancels out in the final noise parameter expressions.

ists between the noise sources of the package and the active device, that is $\overline{N_p J_d} = 0$, one may demonstrate that C_{pd} takes the form

$$C_{pd} = P\overline{N_p N_p^\dagger}P^\dagger + D\overline{J_d J_d^\dagger}D^\dagger. \tag{19}$$

Using the definitions

$$C_p = \overline{N_p N_p^\dagger} \quad C_d = \overline{J_d J_d^\dagger} \tag{20}$$

One may cast (19) into the form

$$C_{pd} = PC_pP^\dagger + DC_dD^\dagger \tag{21}$$

which is (1). For computational purposes, this equation can be reduced to one involving matrices of order 2 only. Thus

$$C_{pd} = C_{ee} + DC_{ie} + C_{ei}D^\dagger + D(C_{ii} + C_d)D^\dagger. \tag{22}$$

The inverse of this operation corresponding to the de-embedding procedure can be derived from (22). Hence

$$C_d = D_i(C_{pd} - C_{ee})D_i^\dagger - C_{ie}D_i^\dagger - D_iC_{ei} - C_{ii} \tag{23}$$

where $D_i = D^{-1}$ and C_{ee}, C_{ei}, C_{ie}, and C_{ii} are submatrices of C_p partitioned in accordance with the format used for Y_p, (6).

We have completed our analysis leading up to (1) and (2) and have presented expressions for the transformation matrices in terms of the package and device admittance parameters. What remains to be done is to obtain expressions for the correlation matrices C_{pd}, C_p, and C_d for the packaged device, the package, and the device as a two-port, respectively. Having done this, we will have completed the connection between the four extrinsic noise parameters $F_{\min}$, Γ_{opt}, and R_n and the noise correlation matrix of the intrinsic device.

The Correlation Matrices

We start with the most simple case, namely, the correlation matrix for the package. We assume that the package contains no active devices, and that it generates thermal noise only. This excludes other sources of noise such as those associated with various magnetic materials. However, we do not rule out the possibility that the package is nonreciprocal.

Since the package is a linear, passive network generating thermal noise only, its noise correlation matrix (admittance form) is expressible in terms of the real part of the admittance matrix as proven by Twiss [9]. Thus

$$C_p = \tfrac{1}{2}(Y_p + Y_p^\dagger). \tag{24}$$

Note that this equation does not require that the package be reciprocal. If the package is reciprocal, $C_p = \text{Re}\{Y_p\}$ where Re { } denotes the real part. We shall assume reciprocity from here on.[3]

We include for sake of completeness, the transformation from the four extrinsic noise parameters of the packaged device to the corresponding admittance correlation matrix. We proceed by first expressing the ABCD or circuit parameter form of the noise correlation matrix in terms of the noise parameters. Let C_A, denote this correlation matrix. It can be shown [2][4] that the elements of this matrix are given by

$$C_{A,11} = R_n \tag{25a}$$

$$C_{A,12} = \frac{F_{\min} - 1}{2} - R_n Y_{s,\text{opt}}^* \tag{25b}$$

$$C_{A,21} = C_{A,12}^* \tag{25c}$$

$$C_{A,22} = R_n |Y_{s,\text{opt}}|^2. \tag{25d}$$

This correlation matrix can be transformed to the desired admittance noise matrix by the Hermitian form

$$C_{pd} = VC_AV^\dagger. \tag{26}$$

Conversely, the reverse transformation is given by

$$C_A = V^{-1}C_{pd}V^{\dagger -1} \tag{27}$$

where the matrix V is expressed in terms of elements of the admittance matrix Y_e as

$$V = \begin{bmatrix} -y_{e,11} & 1 \\ -y_{e,21} & 0 \end{bmatrix}. \tag{28}$$

The extraction of the four extrinsic noise parameters from the matrix C_A, in the reverse transformation, is given by the equations

$$F_{\min} = 1 + 2(C_{A,12} + C_{A,11}Y_{s,\text{opt}}^*) \tag{29a}$$

$$R_n = C_{A,11} \tag{29b}$$

$$Y_{s,\text{opt}} = \sqrt{\frac{C_{A,22}}{C_{A,11}} - \left(\frac{\text{Im } C_{A,12}}{C_{A,11}}\right)^2} + j\left(\frac{\text{Im } C_{A,12}}{C_{A,11}}\right). \tag{29c}$$

We next turn to the correlation matrix of the active two-port. The noise contribution of the two-port consists of two contributions, the noise intrinsic to the device, and the noise associated with resistive or other lossy parasitics. Since the two-port is linear one may show that the noise correlation matrix C_d can be written in its most general form as a superposition of two terms

$$C_d = TNT^\dagger + SN_tS^\dagger \tag{30}$$

The transformation matrices T and S, in general, may be complicated functions of the equivalent circuit parameters (ECPs) of the active device. The correlation matrix N_t represents any thermal noise contributions included with the active device and is known given the ECPs. On the other hand the intrinsic noise matrix N is what is being sought by the de-embedding procedure. Thus, after C_d is derived for the active device from the four extrinsic noise parameters by the procedure described above, N is obtained [10] from (30) as

$$N = T^{-1}(C_d - SN_tS^\dagger)T^{\dagger -1} \tag{31}$$

[3]If the package is at a temperature T then C_p must be multiplied by the factor T/T_o.

[4]There is a typograhpical error in [2]. The asterisk in the (2, 1) element should be transferred to the (1, 2) element in (11).

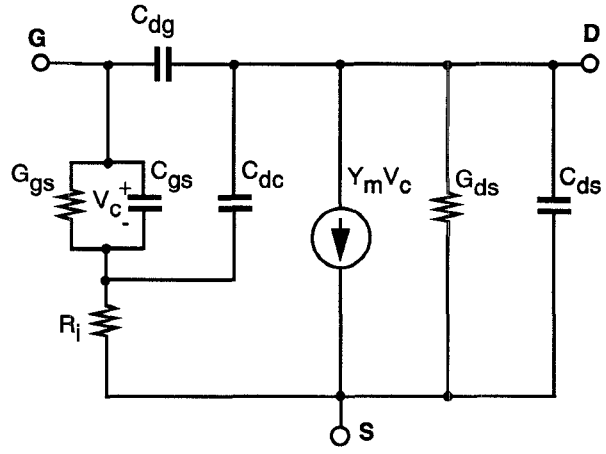

Fig. 5. Definition of intrinsic FET circuit used in noise analysis.

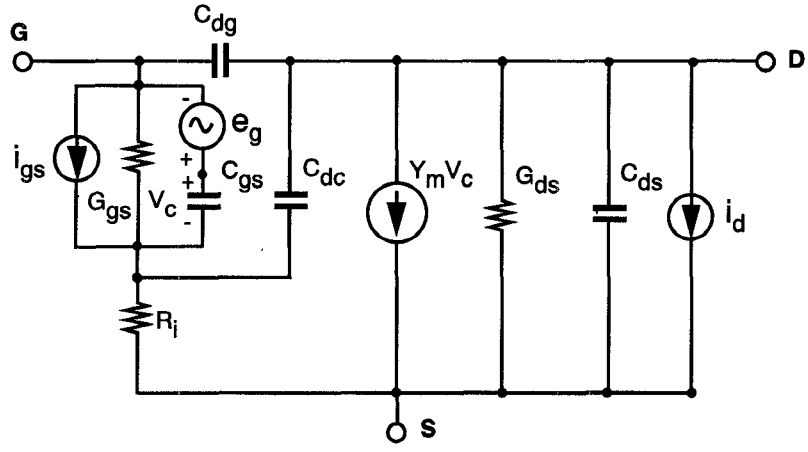

Fig. 6. Noise model of intrinsic FET.

The frequency dependence of the intrinsic noise mechanisms is known.[5] We make use of this fact to predict the noise performance at some frequency differing from that used in the de-embedding. Thus, known N, we may use it in (30), but with values for it and T, S and N_t[6] evaluated at the "new" frequency. The new value for C_d is then inserted into (21), and C_{pd} is calculated, with P, C_p, and D re-evaluated for the new frequency. Then (27), (28), and (29) are used to determine the new values of the extrinsic noise parameters. Thus the de-embedding and analysis procedures are completed.

So far, all of the relations and matrices presented above are independent of the detailed properties of the active device and therefore apply to any active two-port device. However, from here on, the matrix properties, specifically the device two-port admittance Y_d and corresponding noise matrix C_d are device specific.

The small-signal equivalent circuit model for the intrinsic FET is shown in Fig. 5. Note that the parasitic source, gate, and drain resistances are absent as they are considered part of the package. This ensures that the admittance matrix of the package doesn't become singular in the case when only a FET in chip form is being de-embedded. The noise representation is illustrated in Fig. 6. The thermal noise of the gate leakage conductance is represented by a "white" current source i_{gs} across the conductance. The intrinsic noise sources are presented by a white current source i_d across the drain conductance and a white voltage source e_g in series with the gate capacitance [11]. These two sources are correlated with each other but not with the thermal noise source i_{gs}. The intrinsic noise matrix is expressed in terms of these two sources as

$$N = \begin{bmatrix} \overline{e_g e_g^*} & \overline{e_g i_d^*} \\ \overline{i_d e_g^*} & \overline{i_d i_d^*} \end{bmatrix} \tag{32}$$

Note that this matrix is not in admittance form. The calculation of the admittance matrix Y_d and the associated correlation matrix C_d, (30) in terms of the ECPs and the three noise sources is straightforward and described in Appendix I.

[5]For example, in the case of the FET, there is no frequency dependence, unless flicker noise is present.

[6]The matrix N_t, though representing thermal (white) noise sources is frequency dependent because it contains some frequency dependent factors involving the FET ECPs. These factors shape the noise spectra of the thermal noise sources in their transformation to the reference planes corresponding to this matrix.

Summary of Procedure

We shall summarize the entire de-embedding/embedding procedure, step by step. The numbers in parentheses indicate the equation number in the preceding text.

(a) Given the four extrinsic noise parameters $F_{\min}$, $Y_{s,\text{opt}}$, and R_n at some measurement frequency f_m, do the following for this frequency:
(b) Calculate the matrix elements of $\boldsymbol{C}_A$ by (25).
(c) From measurements or simulation calculate package admittance $\boldsymbol{Y}_p$ and partition as per (6).
(d) Calculate device admittance $\boldsymbol{Y}_d$ from its equivalent circuit, for example, for the FET from Fig. 6.
(e) Calculate $\boldsymbol{D}$ by (15).
(f) Calculate $\boldsymbol{V}$ by (28), then C_{pd} by (26).
(g) Calculate $\boldsymbol{C}_p$ by (24) and partition as per (6).
(h) Calculate $\boldsymbol{C}_d$ by (23).
(i) Calculate $\boldsymbol{T}$, $\boldsymbol{S}$, and $\boldsymbol{N}_t$ for the particular device type.
(j) Calculate $\boldsymbol{N}$ by (31).

Change to new frequency f. For this frequency:

(a) Calculate $\boldsymbol{T}$, $\boldsymbol{S}$, and $\boldsymbol{N}_t$
(b) Calculate $\boldsymbol{C}_d$ by (30) using $\boldsymbol{N}$ from step (j) above.
(c) Determine $\boldsymbol{Y}_p$, from simulation or from measurement and partition as per (6).
(d) Calculate $\boldsymbol{Y}_d$ from the equivalent circuit of the device.
(e) Calculate $\boldsymbol{D}$ by (15) then $\boldsymbol{Y}_e$ by (14)
(f) Calcualte $\boldsymbol{C}_p$ by (24) then partition as per (6)
(g) Calculate C_{pd} by (22)
(h) Calculate $\boldsymbol{V}$ by (28) then $\boldsymbol{C}_A$ by (27).
(i) Calculate new extrinsic noise parameters by (29)

Before proceeding to the application of the de-embedding scheme to experimental data, we present next a brief description of the experimental setup used to obtain very accurate noise measurements. We cannot emphasize enough the importance of obtaining accurate noise parameters through the use of a highly redundant set of noise figure measurements and least squares fitting, if the de-embedding scheme is to be successful. The next section describes a measurement system used at our laboratory for ensuring accurate noise data for the de-embedding scheme.

Description of the Noise Measurement Setup

Consistent with our stated objective of presenting a self-contained procedure for noise de-embedding we shall include in this section and in Appendix II, all necessary formulas required to transform the measured noise data to the package input/output reference planes, even though these expressions can be found scattered here and there throughout the literature. This was done to accomodate those readers who may wish to implement the described de-embedding procedure with minimum effort in their own laboratory.

The well-known equation for noise figure of a two-port device in terms of the four noise parameters and the source admittance is shown in (33). Given a minimum set of four noise figure measurements, each at a unique source admittance Y_s, (33) can be used to solve for the four noise parameters at the measurement frequency.

$$NF = F_{\min} + \frac{R_n}{\text{Re}\,\{Y_s\}} |Y_s - Y_{s,\text{opt}}|^2 \tag{33}$$

where NF denotes the noise figure, $F_{\min}$ the minimum noise figure, R_n the noise resistance, and $Y_{s,\text{opt}}$ the optimum source admittance for minimum noise figure. However, because of residual measurement inaccuracies, more than four source admittances are required for the determination of the noise parameters. Usually 10 to 20 source admittances are used for each frequency and the noise parameters are extracted by least squares fitting. We have found that many more source admittances are required for accurate determination of the noise parameters, especially if the noise resistance R_n is low. Therefore, our automated measurement technique employs 90 to 100 source admittances equally spaced over the Smith chart.

A block diagram of the measurement setup used to extract noise parameters is shown in Fig. 7. This setup is a fairly standard single sideband source-pull measurement system employing programmable mechanical tuners, bias tees, and isolators. The measurement setup covers the frequency range from 4 to 26 GHz and uses three sets of isolators (4–8, 8–18, and 18–26 GHz).

The measurement system works in the following manner: The tuner on the gate side of the device is programmed to present the various source admittances to the device under test. This is the heart of the system. The (optional) tuner on the drain side of the device is used to tune the device output for gain. The bias tees provide for dc gate and drain bias to the device under test (DUT). The isolators fill three very important purposes: Firstly, isolator #1 prevents changes in the admittance of the noise source, as it is biased on and off, from affecting the source admittance presented to the DUT during measurement. Secondly, isolator #3 prevents these same changes from affecting the source admittance presented to the noise figure test set during system calibration. (Note: the subsystem containing the DUT enclosed within the dashed lines in Fig. 7, hereafter referred to as the device subsystem, is absent during this calibration step.) Thirdly, during the device measurement isolator #2 insures that the gain measured by the noise figure meter is the available gain of the device subsystem. Inclusion of isolator #2 in the measurement setup eliminates the need for a noise figure correction arising from any mismatch after the drain bias tee (looking back to the DUT). We included isolator #2 for convenience only since the measured noise figure could be corrected for output mismatch by the method described in [12]. We should add that our use of three isolators to avoid mismatch correction is valid provided that the isolators are "sufficiently" well matched—not a difficult condition to satisfy.

During the device measurement step, the noise figure of the device subsystem is measured. De-embedding to

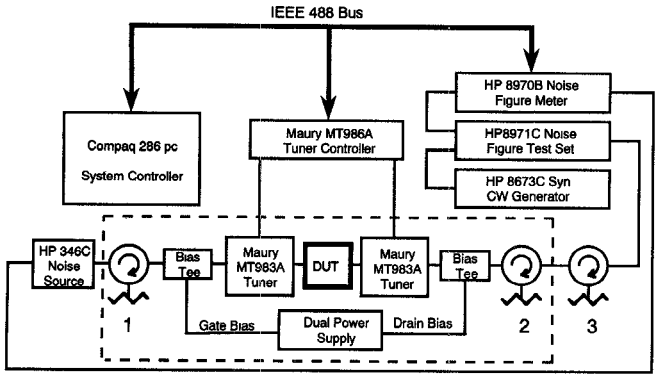

Fig. 7. Test setup for automated measurement of noise parameters.

the reference plane of the DUT and extraction of the four noise parameters is done immediately after all source admittance noise measurements are complete. De-embedding of the measured noise figure to the DUT reference plane is accomplished through the use of the cascade noise figure formula

$$NF_m = NF_1 + \frac{NF_2 - 1}{G_1} + \frac{NF_3 - 1}{G_1 G_2} + \cdots \quad (34)$$

where NF_m denotes the noise figure of a cascaded system, and NF_k and G_k the noise figure and available gain, respectively, of the kth two-port.

One may simplify the measurement setup to three cascaded two-ports by combining the isolator, bias tee, and programmable tuner on each side of the DUT into single two-ports. By solving (34) for NF_2 (DUT noise figure) we have

$$NF_2 = G_1 \left(NF_m - NF_1 - \frac{NF_3 - 1}{G_1 G_2} \right) + 1. \quad (35)$$

The available gains and noise figures needed to solve (35) are calculated from [S]-parameter measurements of the three two ports comprising the noise measurement system. Because the isolators, bias tees, and programmable tuners are all passive components, the noise figures NF_1 and NF_3 can be calculated directly from the [S]-parameter measurements and are related to the available gains G_1 and G_3, and the ambient temperature T of the tuners and isolators as

$$NF_1 = \left(\frac{1}{G_1} - 1 \right) \frac{T}{T_o} + 1 \quad (36a)$$

$$NF_3 = \left(\frac{1}{G_3} - 1 \right) \frac{T}{T_o} + 1 \quad (36b)$$

where $T_o = 290°\text{K}$.

This method of de-embedding the measured noise figure to the DUT reference plane is general for cascaded two-ports. No assumptions are made about the source match of each two-port. The only assumptions underlying (35) are that the first and third two-ports are at the same temperature and are passive, linear, and generate thermal noise only. The equations for calculation of the available gains G_1, G_2, G_3 from the measured S-parameters are given in Appendix II. An equivalent method based on the noise correlation matrix also has been investigated, but has not been adopted because of its somewhat longer execution time on a PC.

After de-embedding of the source admittance noise measurements to the DUT reference plane is completed, the four noise parameters of the DUT are extracted by solution of an overdetermined linear system of equations by the method proposed by Lane [13]. This solution is obtained by rearrangement of (33) into the linear form

$$\text{Re}\,\{Y_{s,i}\}\,NF_i = |Y_{s,i}|^2 x_i - 2\,\text{Im}\,\{Y_{s,i}\}\,x_2 + x_3 + \text{Re}\,\{Y_{s,i}\}\,x_4 \quad (37)$$

where NF_i and $Y_{s,i}$ represent the noise figure and source admittance for the DUT for the ith measurement. Also Re { } and Im { } denote the real and imaginary parts, respectively, of the parameter in braces. The four variables whose solutions are sought are obtained in terms of the four unknown noise parameters by the following relationships

$$x_1 = R_n \quad (38a)$$

$$x_2 = \text{Im}\,\{Y_{s,\text{opt}}\}\,R_n \quad (38b)$$

$$x_3 = |Y_{s,\text{opt}}|^2 R_n \quad (38c)$$

$$x_4 = F_{\min} - 2\,\text{Re}\,\{Y_{s,\text{opt}}\}\,R_n. \quad (38d)$$

The solution of the set of equations (37) is obtained by well-known techniques. In terms of the solutions, we obtain the four noise parameters by inversion of (38). Thus

$$R_n = x_1 \quad (39a)$$

$$\text{Im}\,\{Y_{s,\text{opt}}\} = \frac{x_2}{x_1} \quad (39b)$$

$$\text{Re}\,\{Y_{s,\text{opt}}\} = \sqrt{\frac{x_3}{x_1} - \left(\frac{x_2}{x_1}\right)^2} \quad (39c)$$

$$F_{\min} = x_4 + 2\sqrt{x_1 x_3 - x_2^2}. \quad (39d)$$

Application of De-Embedding Scheme to Experimental Data

The first example is a 0.5 μm by 300 μm gate Raytheon GaAs MESFET. Fig. 8 is the schematic for the "package." In this case, the package consists only of a source inductance L_s and the three FET parasitic resistances R_g, R_d, and R_s of the gate, drain, and source electrodes, respectively. The four port admittance parameters of the package may be obtained by a variety of methods. Note that the inner ports of the package do not share a common reference terminal with the input and output ports. Fig. 9 illustrates the results of the noise modelling. The de-embedding was performed at 10 GHz to determine the internal device noise sources and the solid curves represent the predicted noise performance at other frequencies.

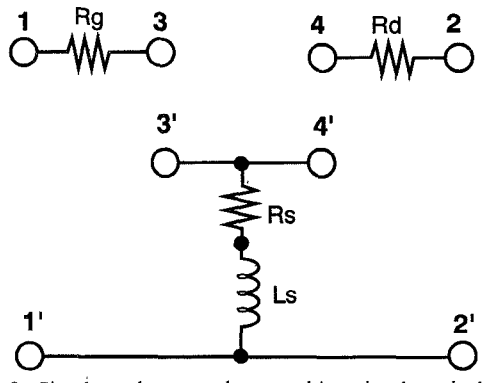

Fig. 8. Simple package topology used in noise de-embedding.

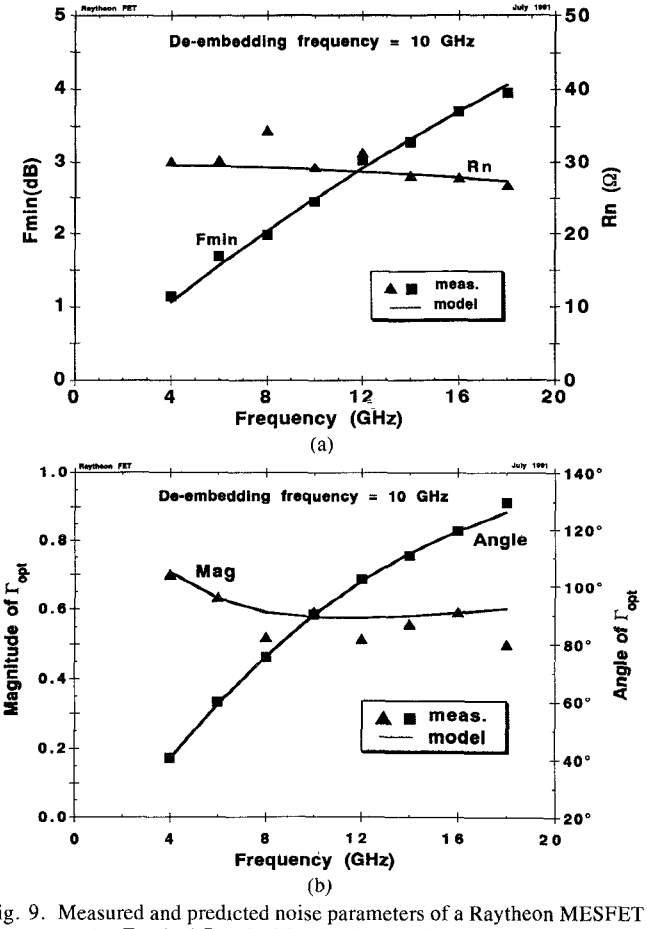

Fig. 9. Measured and predicted noise parameters of a Raytheon MESFET. (a) F_{min} and Rn. (b) Magnitude and phase of Γopt.

Except for some obvious scatter in the measured noise data, particularly in the magnitude of Γ_{opt}, generally satisfactory agreement was obtained between the predicted noise parameters and experiment.

The second example is a Tachonics FET. The package for this device is of the same form as for the Raytheon device, but with different element values. Fig. 10 illustrates the modelled and measured results. For this case the de-embedding took place at 8 GHz. Again, good agreement is obtained for all noise parameters save for the magnitude of the reflection coefficient at the lower end of the frequency band.

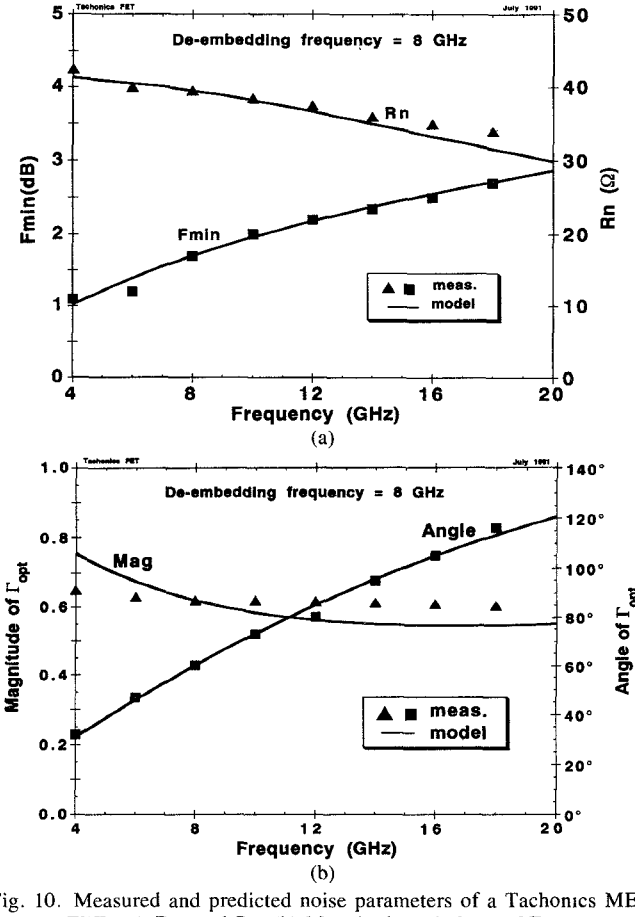

Fig. 10. Measured and predicted noise parameters of a Tachonics MESFET. (a) F_{min} and Rn. (b) Magnitude and phase of Γopt.

The third example is a 0.5 μm by 300 μm pseudomorphic HEMT device fabricated at Raytheon, Fig. 11. This device was characterized and modeled over a wider frequency band. The package topology was the same as the preceding two devices. The de-embedding frequency was 12 GHz. Again, the agreement between the model and experiment is satisfactory. Some scatter in the noise resistance data is evident.

The final example is a Siemens device. In this case, the package toplogy, shown in Fig. 12 is much more complicated than the previous one.[7] In light of the complexity of the package, this example illustrates the power of our general de-embedding technique. Figure 13 demonstrates the comparison between theory and experiment. In this case, the agreement in some of the noise parameters is not as good as in the other two examples, presumably because of the strong frequency dependence of the package as illustrated by the resonance phenomena occurring in the 11–12 GHz range. Because of this resonance we have plotted the angle of the reflection coefficient in modulo 360° for sake of clarity.

We have included in Table I a computer printout for the Siemens device including the equivalent circuit pa-

[7]The four port admittance parameters of this package were obtained from a separate analysis with Super Compact.®

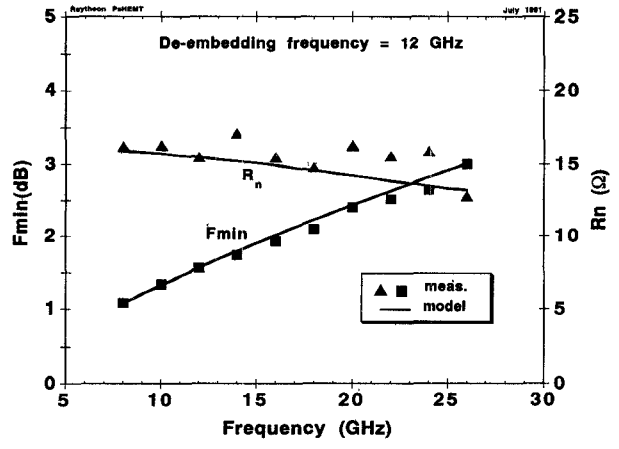

(a)

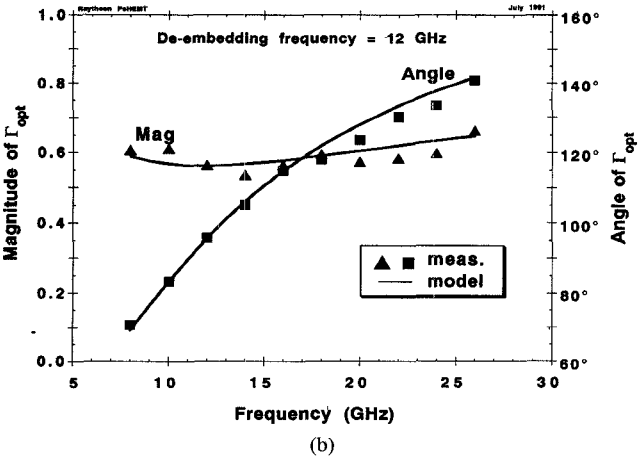

(b)

Fig. 11. Measured and predicted noise parameters of a Raytheon PsHEMT. (a) F_{min} and Rn. (b) Magnitude and phase of Γopt.

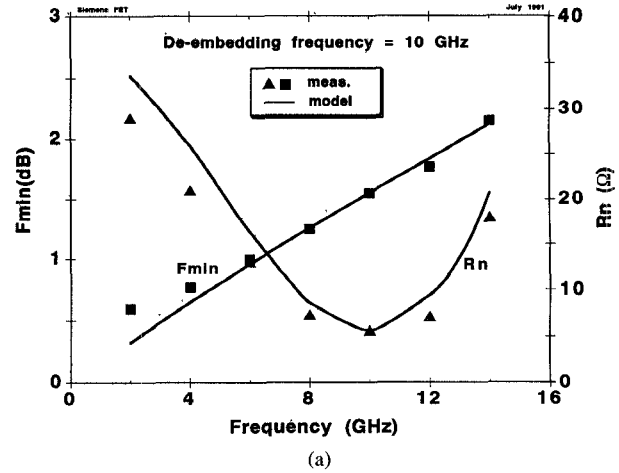

(a)

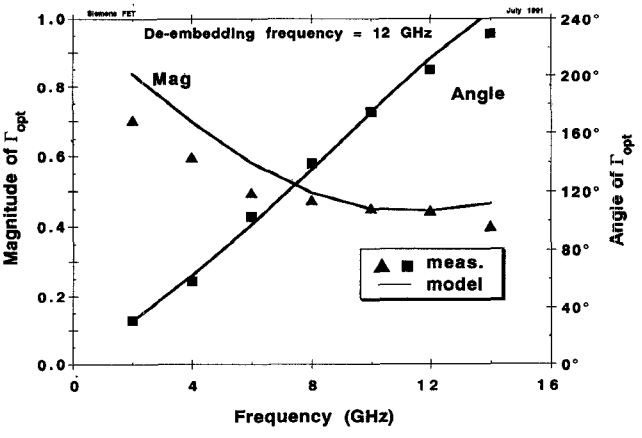

(b)

Fig. 13. Measured and predicted noise parameters of a Siemens MESFET. (a) F_{min} and Rn. (b) Magnitude and phase of Γopt.

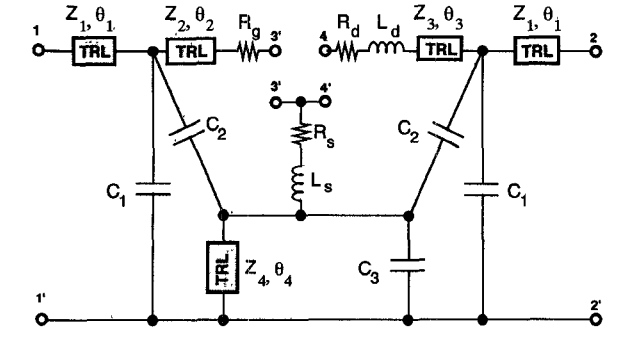

Fig. 12. Complex package topology used in noise de-embedding.

rameter values to serve as a test case for the reader who wishes to implement the de-embedding technique. The transadmittance y_m in Fig. 5 is expressed as

$$y_m = \frac{g_{mo} e^{-j\omega T_1}}{1 + j \dfrac{f}{F_{3\,\mathrm{dB}}}}. \tag{40}$$

Note that the gate, drain, and source parasitic resistances are included in Table I for completeness, but are considered part of the package, Fig. 12.

Summary and Conclusions

A general noise de-embedding procedure for active linear two-ports has been presented which does not require a topological description of the package in which the two-port is embedded. All that is needed is a four-port admittance description of the package which must be passive and generate thermal noise only. The four noise parameters are specified at one frequency and can be calculated for any other frequency provided that the frequency dependence of all noise sources of the active two-port, including their correlation, is known. The de-embedding scheme was applied to several measured FETs and a PsHEMT. Generally speaking, good agreement was obtained with experiment.

A programmable measurement setup was described for automated data acquisition of accurate noise measurements.

TABLE I
EQUIVALENT CIRCUIT PARAMETER VALUES FOR SIEMENS FET, INCLUDING CALCULATED NOISE DATA
Siemens CFY25 Device

Gmo = 67.22 mS	T1 = 0.55 pS	Gds = 5.11 mS	Cgs = 0.368 pF
Cdc = 0.00 pF	Ggs = 0.000 mS	Cdg = 0.040 pF	Cds = 0.050 pF
Ri = 4.269 Ω	Rg = 0.636 Ω	Rs = 5.717 Ω	Rd = 2.238 Ω

F3dB = 1.0E4 GHz

Noise input data at 10.00 GHz:

Fmin = 1.550 dB	Rs, opt = 19.0 Ω	Gamma (mag) = 0.450
Rn = 5.6 Ω	Xs, opt = 2.2 Ω	Gamma (ang) = 174.1 deg

F (GHz)	Fmin (dB)	Rn (ohms)	Rs, opt (ohms)	Xs, opt (ohms)	Gamma (mag)	Gamma (deg)
2.00	0.327	33.6	57.2	164.7	0.839	30.6
4.00	0.649	25.9	30.3	73.4	0.698	62.6
6.00	0.957	16.4	22.3	38.9	0.581	97.2
8.00	1.258	8.6	19.4	18.1	0.495	134.8
10.000	1.550	5.6	19.0	2.2	0.450	174.1
12.00	1.837	9.4	20.5	−12.0	0.445	−148.1
14.00	2.123	20.7	24.5	−26.4	0.464	−114.4

APPENDIX I
DERIVATION OF CORRELATION MATRIX AND ADMITTANCE MATRIX OF AN FET IN TERMS OF INTERNAL NOISE SOURCES AND EQUIVALENT CIRCUIT PARAMETERS

INTRODUCTION

We shall derive the expressions for the noise matrices $\boldsymbol{T}$, $\boldsymbol{S}$, $\boldsymbol{N}$, and N_t in terms of the equivalent circuit parameters (ECPs) of the FET. These matrices are used in (30) and (31) in the text. As a byproduct, an expression for the device admittance matrix Y_d will be obtained.

ANALYSIS

Our first task is to transform the internal noise sources in Fig. 6 to their equivalent external shunt form in Fig. 2. For this purpose we define noise vectors for the internal and external sources in matrix form as follows:

$$\boldsymbol{n} = \begin{bmatrix} e_g \\ i_d \end{bmatrix} \quad \boldsymbol{J}_d = \begin{bmatrix} j_3 \\ j_4 \end{bmatrix} \quad \boldsymbol{i}_{gs} = [i_{gs}] \tag{I-1}$$

from which we may write

$$\boldsymbol{J}_d = \boldsymbol{T}\boldsymbol{n} + \boldsymbol{F}\boldsymbol{i}_{gs} \tag{I-2}$$

where the elements of the transformation matrices $\boldsymbol{T}$ and $\boldsymbol{F}$ can be derived from circuit theory. The expressions for these elements are given below:

$$T_{11} = \frac{j\omega C_{gs}}{1 + Y_{gs}Z_i} \tag{I-3a}$$

$$T_{12} = 0 \tag{I-3b}$$

$$T_{21} = g_m - \frac{j\omega C_{gs}Z_i}{1 + Y_{gs}Z_t}(Y_m + j\omega C_{dc}) \tag{I-3c}$$

$$T_{22} = 1 \tag{I-3d}$$

and

$$F_1 = \frac{1}{1 + Y_{gs}Z_i} \tag{I-4a}$$

$$F_2 = -\frac{Z_t}{1 + Y_{gs}Z_t}(Y_m + j\omega C_{dc}) \tag{I-4b}$$

where

$$Z_t = \frac{R_i}{1 + j\omega C_{dc}R_t} \tag{I-5}$$

$$Y_{gs} = G_{gs} + j\omega C_{gs}. \tag{I-6}$$

The device correlation matrix $\boldsymbol{C}_d$ is defined by the expression

$$\boldsymbol{C}_d = \overline{\boldsymbol{J}_d\boldsymbol{J}_d^\dagger} = \boldsymbol{T}\boldsymbol{N}\boldsymbol{T}^\dagger + \boldsymbol{S}\boldsymbol{N}_t\boldsymbol{S}^\dagger \tag{I-7}$$

where

$$\boldsymbol{N} = \overline{\boldsymbol{n}\boldsymbol{n}^\dagger} \tag{I-8}$$

$$\boldsymbol{N}_t = \boldsymbol{F}\overline{\boldsymbol{i}_{gs}\boldsymbol{i}_{gs}^\dagger}\boldsymbol{F}^\dagger = \frac{T}{T_o}G_{gs}\overline{\boldsymbol{F}\boldsymbol{F}^\dagger} \tag{I-9}$$

since $\overline{\boldsymbol{i}_{gs}\boldsymbol{i}_{gs}^\dagger} = (T/T_o)G_{gs}$.[8] The matrix $\boldsymbol{S}$ in this case is simply the identity matrix.

The elements of the admittance matrix $\boldsymbol{Y}_d$ of the device are given by

$$Y_{d11} = \frac{Y_{gs}}{1 + Y_{gs}Z_t} + j\omega C_{dg} \tag{I-10}$$

$$Y_{d12} = -\frac{j\omega C_{dc}Y_{gs}Z_i}{1 + Y_{gs}Z_i} - j\omega C_{dg} \tag{I-11}$$

[8]Recall that we have normalized all noise noises to $2kT_oB$. The factor T/T_o accounts for the fact that the leakage conductance G_{gs} may be at a temperature T. Note that we are tacitly assuming in this example that G_{gs} represents thermal noise only.

$$Y_{d21} = \frac{Y_m - j\omega C_{dc} Y_{gs} Z_i}{1 + Y_{gs} Z_i} - j\omega C_{dg} \tag{I-12}$$

$$Y_{d22} = j\omega C_{dc} Z_i \left[\frac{\left(\frac{1}{R_i} + Y_{gs} \right) - Y_m}{1 + Y_{gs} Z_i} \right] + G_{ds} + j\omega(C_{ds} + C_{dg}). \tag{I-13}$$

This completes the analysis.

Appendix II
Derivation of Formulas Relevant to Noise Measurement System

We develop below the equations for expressing the available gains of the various "gain" blocks in our measurement setup in terms of the mismatch or reflection coefficients between blocks.

Fig. 14 shows in abbreviated form three essential gain blocks designated by the available "gains" G_a, G_b, and G_c and associated S-parameters S_a, S_b, S_c. The block designated b denotes the device under test (DUT), whereas the blocks denoted by a and c represent, respectively, the aggregate of blocks preceding and following the DUT. Let Γ_s, Γ_a, Γ_b, and Γ_c denote the reflection coefficients at the illustrated reference planes. These coefficients are calculated from the measured S-parameters of the various gain blocks and the source reflection coefficient Γ_s. Thus we have

$$\Gamma_a = S_{22,a} + \frac{S_{12,a} S_{21,a} \Gamma_s}{1 - \Gamma_s S_{11,a}} \tag{II-1a}$$

$$\Gamma_b = S_{22,b} + \frac{S_{12,b} S_{21,b} \Gamma_a}{1 - \Gamma_a S_{11,b}} \tag{II-1b}$$

$$\Gamma_c = S_{22,c} + \frac{S_{12,c} S_{21,c} \Gamma_b}{1 - \Gamma_b S_{11,c}}. \tag{II-1c}$$

The available gains are expressed in terms of these reflection coefficients as

$$G_a = \frac{|S_{21,a}|^2 (1 - |\Gamma_s|^2)(1 - |\Gamma_a^*|^2)}{|(1 - \Gamma_s S_{11,a})(1 - \Gamma_a^* S_{22,a}) - \Gamma_s \Gamma_a^* S_{12,a} S_{21,a}|^2} \tag{II-2a}$$

$$G_b = \frac{|S_{21,b}|^2 (1 - |\Gamma_a|^2)(1 - |\Gamma_b^*|^2)}{|(1 - \Gamma_a S_{11,b})(1 - \Gamma_b^* S_{22,b}) - \Gamma_a \Gamma_b^* S_{12,b} S_{21,b}|^2} \tag{II-3b}$$

$$G_c = \frac{|S_{21,c}|^2 (1 - |\Gamma_b|^2)(1 - |\Gamma_c^*|^2)}{|(1 - \Gamma_b S_{11,c})(1 - \Gamma_c^* S_{22,c}) - \Gamma_b \Gamma_c^* S_{12,c} S_{21,c}|^2}. \tag{II-4c}$$

In the text, G_a, G_b, and G_c are identified with G_1, G_2, and G_3 respectively.

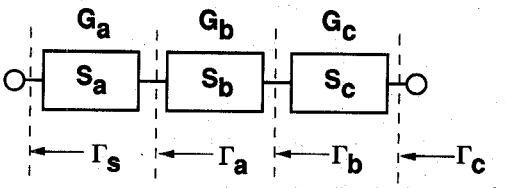

Fig. 14. Relevant to calculation of available gain.

References

[1] H. A. Haus and R. B. Adler, *Circuit Theory of Linear Noisy Networks*. New York: Technology Press of MIT and Wiley, 1959.

[2] H. Hillbrand and P. H. Russer, "An efficient method for computer aided noise analysis of linear amplifier networks," *IEEE Trans. on Circuits Syst.*, vol. CAS-23, pp. 235–238, April 1976.

[3] H. Hillbrand and P. H. Russer, "Rauschanalyse von linearen netzwerken," *Wiss. Ber. AEG-Telefunken*, vol. 49, pp. 127–138, 1976.

[4] V. Rizzoli and A. Lipparini, "Computer-aided noise analysis of linear multiport networks of arbitrary topology," *IEEE Trans. Microwave Theory Tech.*, vol. MTT-33, pp. 1507–1512, Dec. 1985.

[5] S. Heinen, J. Kunisch, and I. Wolff, "A unified framework for computer-aided noise analysis of linear and nonlinear microwave circuits," in *IEEE MTT-S Int. Microwave Symp. Dig.*, pp. 1217–1220, 1991.

[6] V. Rizzoli, F. Mastri, and C. Cecchetti, "Computer-aided noise analysis of MESFET and HEMT mixers," *IEEE Trans. on Microwave Theory and Tech.*, vol. 37, pp. 1401–1411, Sept. 1989.

[7] A. Riddle, "Extraction of FET model noise parameters from measurement," in *IEEE MTT-S Int. Microwave Symposium Dig.*, 1991, pp. 1113–1116.

[8] R. A. Pucel, H. A. Haus, and H. Statz, "Signal and noise properties of gallium arsenide microwave field-effect transistors," in *Advances in Electronics and Electron Physics*, vol. 38. New York: Academic Press, 1975.

[9] R. Q. Twiss, "Nyquist's and Thevenin's theorems generalized for nonreciprocal linear networks," *J. Appl. Phys.*, vol. 26, pp. 599–602, May 1955.

[10] U. L. Rohde, "New nonlinear noise model for MESFETs including MM-wave application," in *Dig. 1990 IEEE Integrated Nonlinear Microwave and Millimeterwave Circuits Workshop*, Duisburg University, Duisburg, Germany, p. 243.

[11] M. W. Pospieszalski, "Modeling of noise parameters of MESFET's and MODFET's and their frequency and temperature dependence," *IEEE Trans. Microwave Theory Tech.*, vol. 37, pp. 1340–1350, Sept. 1989.

[12] K. Mishima and Y. Sawayama, "Comments on simultaneous determination of device noise and gain parameters through noise measurements only," *Proc. IEEE*, vol. 70, pp. 100–101, Jan. 1982.

[13] R. Q. Lane, "The determination of device noise parameters," *Proc. IRE*, vol. 57, pp. 1461–1462, Aug. 1969.

Robert A. Pucel (S'48–M'56–SM'64–F'79–LF'92) received his Sc.D. degree in 1955 from the Massachusetts Institute of Technology in the field of electrical communications. In 1955, he rejoined the Research Division of the Raytheon Company as a staff member specializing in the area of solid-state device research. From 1965 to 1970 he was the project manager of the Microwave Semiconductor Devices and Integrated Circuits Program. This has evolved into the Monolithic Microwave Integrated Circuits Program. Dr. Pucel is now a Consulting Scientist in this program and a project manager in numerical device simulation of microwave semiconductor devices.

His research has encompassed both theoretical and experimental studies of most microwave semiconductor devices, including their signal and noise properties. His most recent work is in the field of monolithic microwave integrated circuits (MMICs) in the area of device modeling and its CAD implementation. He has lectured and published extensively on these topics.

Dr. Pucel is a co-recipient of the 1976 Microwave Prize granted by the MTT Society and he was the National Lecturer for this Society for the 1980–1981 period on the subject of GaAs MMICs. In this role, he has lectured in the United States, Canada, Europe, the Middle East, and Asia, including Japan and the People's Republic of China.

In 1988 Raytheon granted him its most prestigious award, the Excellence in Technology Award during its first year of operation. The MTT Society honored Dr. Pucel in 1990 with its highest recognition, the Microwave Career Award. Dr. Pucel is the editor of the IEEE reprint volume on Monolithic Microwave Integrated Circuits and is a member of the Editorial Board of the MTT Society.

Wayne Struble was born in Zeeland, Michigan in 1959. He received the Bachelor's and Master's degrees in electrical engineering from Michigan Technological University in 1981 and 1983, respectively.

In 1983 he joined the Equipment Division Laboratory of Raytheon Company as a GaAs MMIC design engineer where he was active in the design and testing of low noise amplifiers, phase shifters, power amplifiers and attenuators for microwave phased array applications. In 1988 he transferred to the Research Division of Raytheon where he expanded his work to include both linear and nonlinear GaAs device characterization and modeling. Today, he continues to work in this division in the GaAs MMIC area. His interests include noise characterization and measurement techniques of microwave components and GaAs device modeling including both linear and nonlinear circuit models.

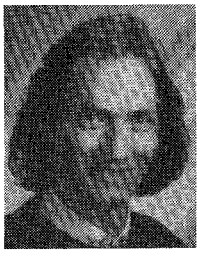

Robert Hallgren (S'85–M'88) received the B.S.E.E. degree from the University of Colorado (Boulder) in 1981, and the Masters and Ph.D. degrees from Cornell University in 1985 and 1988, respectively.

From 1981 to 1984 he was with the Spokane Instrument Division of Hewlett-Packard, and spent two summers at the Microwave Technology Division of HP in Santa Rosa, CA in 1986 and 1987. From 1988 to 1990 he was a senior scientist at the Raytheon Research Division in Lexington, MA working on models for advanced microwave semiconductor devices. Since 1990 he has been with the Electromagnetics Institute at the Technical University of Denmark investigating models for advanced and optical devices.

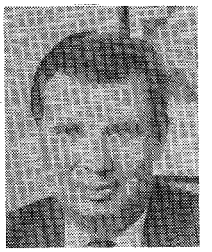

Ulrich L. Rohde studied electrical engineering and radio communications at the universities of Munich and Darmstadt, West Germany, he holds a Ph.D. in electrical engineering and an Sc.D. (hon.) in radio communications.

He is president of Compact Software, Chairman of Synergy Microwave Corp., and a partner of Rohde & Schwarz, Munich, West Germany, a multinational company specializing in advanced test and radio communications systems. Previously, he was the business area director for Radio Systems of RCA, Government Systems Division, Camden, New Jersey, responsible for implementing communications approaches for military secure and adaptive communications.

In 1990 Dr. Rohde was appointed Visiting Research Professor at New Jersey Institute of Technology, Department of Electrical Engineering, Newark, NJ. Dr. Rohde is also a member of the staff at George Washington University and as an adjunct professor teaching in the Electrical Engineering and Computer Sciences departments gave numerous lectures worldwide regarding communications theory and digital frequency synthesizers. In addition, he held the position of Professor of Electrical Engineering at the University of Florida, Gainesville, teaching radio communications courses.

Dr. Rohde has published more than 50 scientific papers in professional journals, as well as four books: *Communications Receivers: Principles and Design*, (McGraw Hill, 1987); *Digital PLL Frequency Synthesizers: Theory and Design*, (Prentice-Hall 1983); *Transistoren bei hoechsten Frequenzen*, in German, (1965), (on microwave transistors). His latest book, *Microwave Circuit Design Using Linear and Nonlinear Techniques*, with co-authors George Vendelin and Anthony W. Pavio was published by John Wiley & Sons, NY, January 1990.